Cell, Vol. 117, 373–386, April 30, 2004, Copyright ©2004 by Cell Press

Nkx2-5 Pathways and Congenital Heart Disease: Loss of Ventricular Myocyte Lineage Specification Leads to Progressive Cardiomyopathy and Complete Heart Block

Mohammad Pashmforoush,[1,7] Jonathan T. Lu,[1,7] Hanying Chen,[6] Tara St. Amand,[1] Richard Kondo,[1] Sylvain Pradervand,[1] Sylvia M. Evans,[1] Bob Clark,[2] James R. Feramisco,[1] Wayne Giles,[1] Siew Yen Ho,[3] D. Woodrow Benson,[4] Michael Silberbach,[5] Weinian Shou,[6] and Kenneth R. Chien[1,*]

[1]UCSD Institute of Molecular Medicine
University of California San Diego School of Medicine
La Jolla, California 92093
[2]University of Calgary
School of Medicine
Calgary, Alberta
Canada
[3]National Heart & Lung Institute
Imperial College and Royal Brompton Hospital
London
England
[4]University of Cincinnati
Cincinnati, Ohio 45221
[5]University of Oregon Health Sciences Center
Portland, Oregon 97239
[6]Herman B Wells Center for Pediatric Research
Indiana University School of Medicine
Indianapolis, Indiana 46202

Summary

Human mutations in *Nkx2-5* lead to progressive cardiomyopathy and conduction defects via unknown mechanisms. To define these pathways, we generated mice with a ventricular-restricted knockout of Nkx2-5, which display no structural defects but have progressive complete heart block, and massive trabecular muscle overgrowth found in some patients with *Nkx2-5* mutations. At birth, mutant mice display a hypoplastic atrioventricular (AV) node and then develop selective dropout of these conduction cells. Transcriptional profiling uncovered the aberrant expression of a unique panel of atrial and conduction system-restricted target genes, as well as the ectopic, high level BMP-10 expression in the adult ventricular myocardium. Further, BMP-10 is shown to be necessary and sufficient for a major component of the ventricular muscle defects. Accordingly, loss of ventricular muscle cell lineage specification into trabecular and conduction system myocytes is a new mechanistic pathway for progressive cardiomyopathy and conduction defects in congenital heart disease.

Introduction

Congenital heart disease can result in the progressive cardiomyopathy and life-threatening electrophysiological disorders that often continue long after the surgical correction of the structural defects. While a number of mutations in cardiac transcription factors have now been linked to genetic forms of congenital heart disease (Bruneau, 2002; Epstein, 2001; Garg et al., 2003), the disease pathways that drive the onset of specific cardiac muscle cell phenotypes, defects in trabeculation, compaction, septation, and the formation of specialized conduction system myocytes remain unclear. Human mutations in *Nkx2-5*, a cardiac homeobox gene, predominantly function in a dominant-negative fashion and cause a diverse set of congenital heart malformations that include septal defects, cardiomyopathy, outflow tract defects, hypoplastic left heart, and associated arrhythmias (Benson et al., 1999; Elliott et al., 2003; Goldmuntz et al., 2001; Gutierrez-Roelens et al., 2002; Schott et al., 1998). The complexity of the congenital cardiac malformations associated with human *Nkx2-5* mutations suggests a potential role for Nkx2-5 at later stages of cardiac morphogenesis during the development of discrete atrial, ventricular, and conduction cell lineages. Nkx2-5 is expressed in the primary and secondary heart fields and plays a pivotal role in the early steps of mammalian cardiogenesis (for a review, see Harvey et al., 2002). Mice that harbor a complete global knockout of Nkx2-5 display early embryonic lethality and defects in cardiac looping morphogenesis, consistent with a role for Nkx2-5 in the early stages of cardiogenesis (Lyons et al., 1995; Tanaka et al., 1999). The central challenge is to delineate the molecular mechanisms that link the loss of Nkx2-5 with these cardiac disease phenotypes, which could simply reflect late, secondary effects of an early requirement of Nkx2-5 in the primary and secondary heart fields. Alternatively, these defects might reflect a later requirement for Nkx2-5 within specific cardiac muscle lineages during cardiac chamber maturation.

To address this problem, we have generated mice that harbor a ventricular muscle cell-restricted knockout of Nkx2-5 that escape the early, complete embryonic lethality found in the global knockout mouse lines. Utilizing these *Nkx2-5* "*floxed*" allele mice, we now have identified an intrinsic role for this cardiac restricted homeobox gene in the formation and maturation of the AV nodal and ventricular myocyte lineages. Multiple lines of evidence document that the loss of Nkx2-5-derived cues leads to defects in the morphogenesis, maturation, and specification of the AV nodal and working myocyte cell lineages. Taken together, these studies identify the mechanistic pathways and key downstream target genes that are linked to the muscle and conduction system defects and have important implications for understanding the pathways for cardiomyopathy and arrhythmogenesis in human congenital heart disease.

Results

Generation of Ventricular Restricted Nkx2-5-Deficient Mice

Nkx2-5 floxed allele mice were generated (Figure 1; for further details, see Supplemental Data at http://www.

*Correspondence: kchien@ucsd.edu
[7]These authors contributed equally to this work.

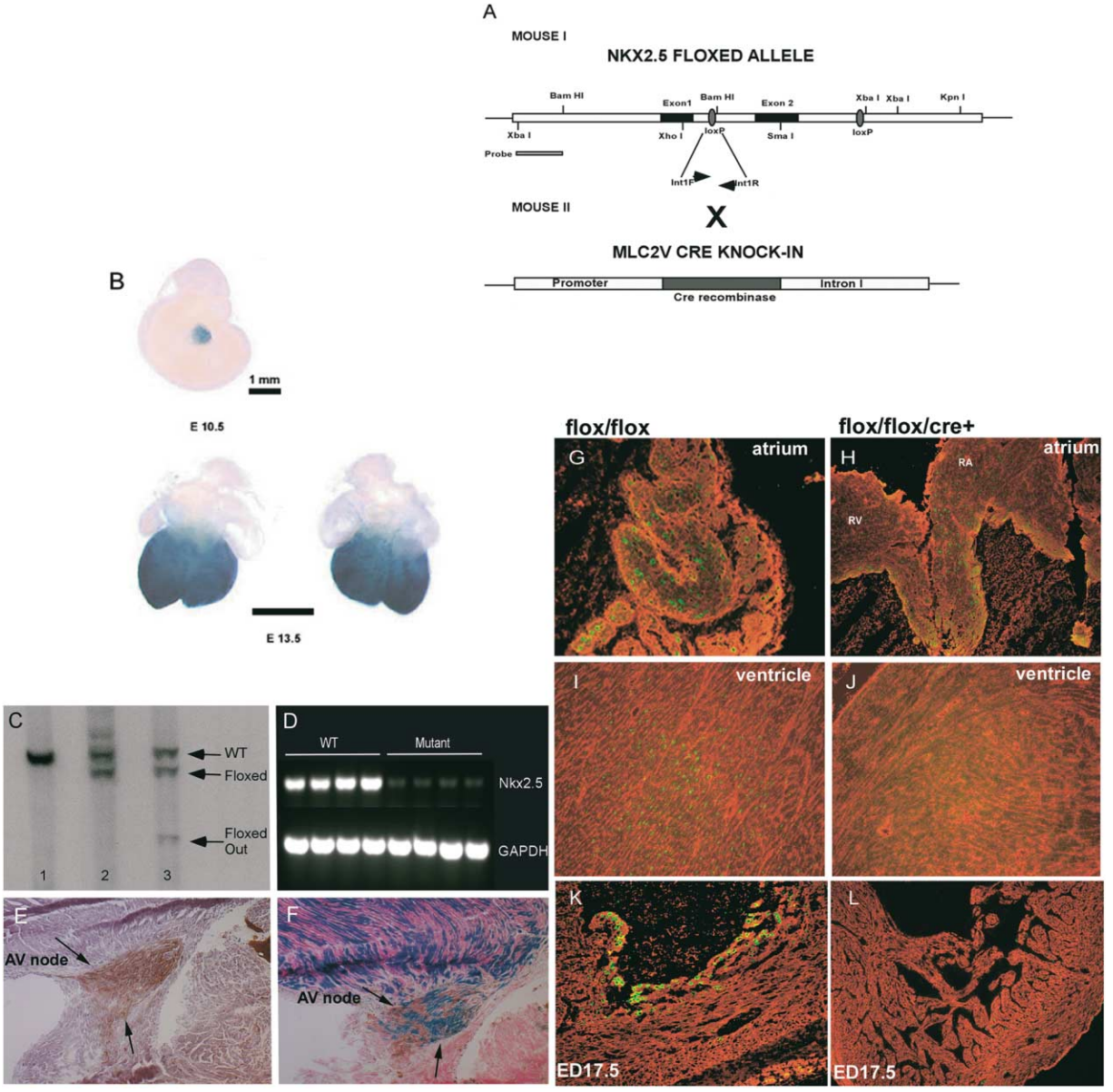

Figure 1. Gene Targeting and Validation of Nkx2-5 Ventricular Restricted Knockout Mice

(A) Targeting Vector depicting the locations of *loxP* site flanking exon 2 of murine *Nkx2-5* gene. As illustrated, MLC2v-cre knockin mice (mouse I) were crossed with mice (mouse II) carrying floxed *Nkx2-5* alleles to generate tissue-specific deletion of Nkx2-5.

(B) Whole-mount LacZ reporter gene expression in the ED 13.5 heart when MLC2v-cre mouse is crossed with R26R Reporter mice.

(C) Southern Blot using ^{32}P labeled 5′ probe and XbaI digest. Lane 1 is total RNA isolated from a wild-type heart. Lane 2 shows lung tissue derived from a mouse whose genotype was heterozygous for floxed allele and positive for MLC2v-cre. Lane 3 is heart tissue from the same mouse as lane 2.

(D) RT-PCR of *Nkx2-5* message from RNA derived from three wild-type hearts and three mutant hearts. Bottom row shows the RT-PCR of GAPDH of the same samples.

(E) Acetylcholinestrase (AChE) activity stain of a 10-day-old R26R reporter mouse crossed with MLC2v-cre, showing staining in the AVN, counterstained with hematoxylin.

(F) Same as above, but double stained for both β-galactosidase and AChE.

(G) and (H) show immunofluorescent staining using anti-Nkx2-5 (green) and anti-α-actinin (red) antibodies in WT and mutant atria.

(I) and (J) show the immunofluorescent staining pattern in WT and mutant ventricles. Nkx2-5 expression is intact in mutant atria, but absent in the ventricle compared to control.

(K) and (L) show immunofluorescent staining pattern in WT and mutant ventricle at ED 17.5, again showing intact Nkx2-5 expression in WT ventricle but nearly absent in mutant ventricle.

cell.com/cgi/content/full/117/3/373/DC1) and crossed into the well-characterized myosin light chain-2v (MLC2v) *cre* recombinase knockin mouse line (Hirota et al., 1999; Ruiz-Lozano and Chien, 2003). The *Nkx2-5 floxed* allele was designed such that the loxP sites flank exon 2, which contains the homeobox domain (Figure 1A). Fig-

ures 1B and 1C show that the MCL2v-cre-mediated recombination of *floxed* allele is efficient and tissue specific. We demonstrated the specificity and the efficiency of MLC2v-cre-mediated recombination for the working myocardium and the conduction system by crossing MLC2v-cre mouse line with the R26R reporter mouse; Figures 1E and 1F show the acetylcholinesterase (AChE) activity stain of the AV node and the lacZ counterstained adjacent section in the resultant progeny; greater than 50% of cells in the AV nodes were positive for lacZ expression, indicating the depletion of Nkx2-5 expression within this tissue.

Neonatal Ventricular Restricted *Nkx2-5* Mutant Mice Lack Atrial Septal Defects and Related Congenital Heart Disease Phenotypes

Adult and neonatal mutant mice and their *flox*/wt and *flox/flox* littermates were exhaustively analyzed by serial section histology, rendering no evidence of atrial or ventricular septal defects (data not shown). Real-time RT-PCR revealed greater than a 90% decrease in Nkx2-5 expression in the adult *flox/flox*/cre$^+$ ventricles (data not shown, see Figure 1D for semiquantitative RT-PCR results). In contrast, RNA isolated from *flox/flox* and *flox/flox/cre*$^+$ atria displayed similar levels of *Nkx2-5* transcripts (not shown). Immunostaining of Nkx2-5 protein in *flox/flox/cre*$^+$ hearts showed little immunoreactivity in the ventricle, while atrial expression was preserved (Figures 1G–1J). Embryonic left ventricles similarly showed a significantly decreased Nkx2-5 immunoreactivity (Figures 1K and 1L). These studies revealed that the efficiency of MLC2v-cre-mediated recombination was about 80%–90% as previously described (Chen et al., 1998; Hirota et al., 1999). Quantification of *Nkx2-5* mRNA and protein levels revealed no difference between wild-type (WT) and homozygous *floxed* (*flox/flox*) mice (data not shown).

Conduction System Disease in Ventricular Restricted Nkx2-5-Deficient Mice

Neonatal Nkx2-5-deficient mice displayed no arrhythmias by surface ECG. Recordings obtained by subcutaneous telemetry transmitters from young mutant mice (12 weeks) revealed first degree AV block and marked QRS prolongation when compared to wild-type mice (Figures 2A–2C). However, at a later stage (6–12 months), advanced AV conduction block progressing to complete heart block became evident in 50% of mutant mice, while *flox/flox* mice of the same age were unaffected (data not shown). Furthermore, these results are consistent with a ventricular origin, as opposed to atrial, of the central conduction system. Our mouse model recapitulates the clinical syndrome of progressive AV block seen in patients with *Nkx2-5* mutations, but without the associated congenital cardiac malformations such as atrial and ventricular septal defects.

To determine if young mutant mice harbor a central conduction system defect that might not be readily detectable via surface ECG, microelectrode EP studies were conducted utilizing Langendorff heart preparations. In the *flox/flox/cre*$^+$ mice, there were clear defects in the electrophysiological function of the AV node and intersecting His bundle (n = 3), manifested as a selective prolongation of the A-H interval and a marked decrease in the His deflection signal (data not shown), indicating a specific conduction system defect. We then utilized a combination of trichrome, immunohistochemistry, and AChE activity staining (Anderson et al., 1974; Crick et al., 1999a, 1999b) to define and analyze the AV node and the distal conduction system. Histochemical analysis of AChE activity (Figures 2H–2K and 3A, 3D, 3G, and 3J) and trichrome staining were performed on serial sections throughout the entire AV node and His bundle. In day 1 neonates, surface ECGs did not suggest a significant conduction system abnormality, and the overall heart size in the *flox/flox/cre*$^+$ mice was only modestly larger than their *flox/flox* littermates with variable penetrance. Analysis of serial sections through these hearts failed to demonstrate any atrial or ventricular septal defects. In contrast, the AV node and the His bundle appeared smaller in *flox/flox/cre*$^+$ mice (Figures 2F and 2G). The expression of the Cx40 was relatively preserved in the conduction system. The adult *flox/flox/cre*$^+$ mice showed a markedly smaller and atrophic conduction system that was age dependent (Figures 2H–2K).

Progression of AV Block in Ventricular Restricted *Nkx2-5* Mutant Mice Is Associated with Cardiomyocyte Dropout and Fibrosis in the Central Conduction System

Conduction cells are modified forms of cardiomyocytes and similarly possess muscle cell sarcomeric structures (Anderson et al., 1974). To determine the overall health and cellular composition of the AV node and His bundle, we utilized a combination of anatomical landmarks and AChE activity staining to define the proper boundaries of the AV node. Figure 3 (panels B, C, E, F, H, I, K, and L) shows the immunostaining of the AV node and the His bundle using anti-sarcomeric α-actinin (rhodamine, red) and anti-Nkx2-5 N terminus (FITC, green) antibodies. We noted that a distinct feature of the conduction system in the mouse was the marked upregulation of Nkx2-5 (Thomas et al., 2001). Our data indicate that in the central and distal conduction system (including the Purkinje cells), Nkx2-5 immunoreactivity was more abundant compared to the surrounding working myocardium. This pattern was present during late embryonic development when a discernable AV node was seen (ED 17.5, data not shown) and extended into adult life. In contrast, in *flox/flox/cre*$^+$ mice, there was only sporadic Nkx2-5 nuclear staining in the conduction system (Figure 3M), consistent with a high degree of cre-mediated recombination in the conduction system. Prior studies have shown a relatively higher expression of MLC2v in the mouse conduction system (Franco and Icardo, 2001). A systematic serial section comparison of the proximal to distal AV node and the His bundle using α-actinin immunostaining was performed. Mice homozygous for the Nkx2-5 ventricular restricted KO had atrophic, disorganized conduction tissue that was significantly smaller than that of their *flox/flox* littermates. We serially sectioned *flox/flox/cre*$^+$ (n = 8) and *cre*$^-$ (*flox/flox, flox/wt*; n = 8) littermates and examined their AV node. Using AChE, we found that both the intensity and area of staining were diminished in *flox/flox/cre*$^+$

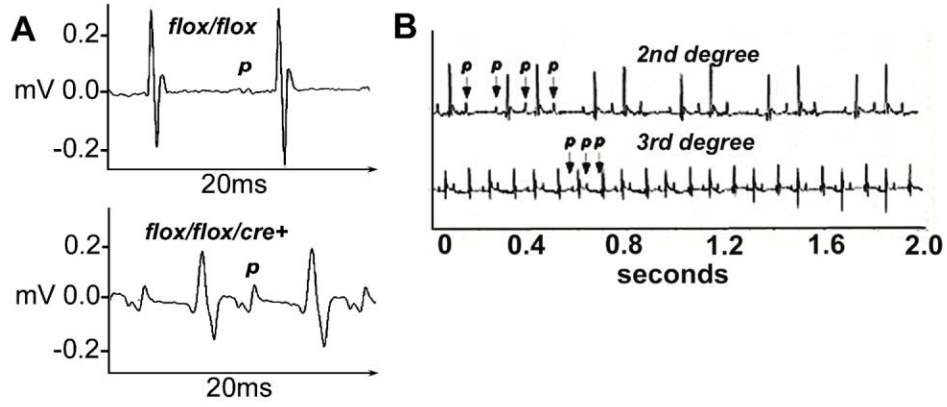

C

	flox/flox	flox/flox/cre+
HR (bpm)	435 +/- 142	365 +/- 194
PR interval (mS)	36.5 +/- 4.7*	45.3 +/- 6.4*
QRS interval (mS)	13.1 +/- 2.7*	17.5 +/- 4.3*
QTc interval (mS)	44.2 +/- 5.7	46.5 +/- 7.9

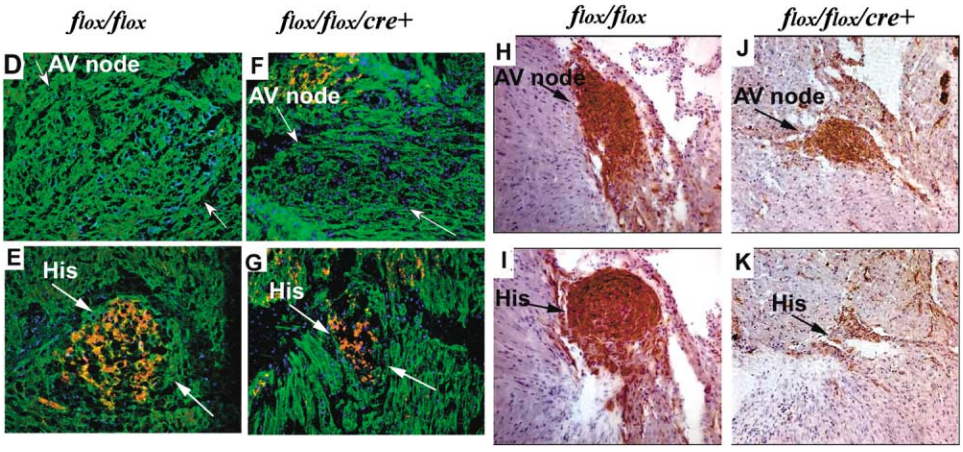

Figure 2. Conduction System Function and Morphology in Nkx2-5 Conditional KO Mice

(A) Adult *flox/flox/cre*$^{+}$ mice at 14–30 weeks displayed PR and QRS prolongation compared to *flox/flox* littermates.

(B) Older mice developed intermittent or persistent second- and third-degree heart block on telemetry. Upper ECG tracing shows second-degree heart block, and later, the same mouse developed third-degree heart block.

(C) A summary of surface ECG parameters in adult *flox/flox* and *flox/flox/cre*$^{+}$ mice ($n = 5$ in each group). The asterisks indicate statistical significance at $p < 0.01$.

(D–I) Frozen sections (5 μM thick) of the day 1 neonatal hearts were analyzed by immunofluorescent staining using anti-Cx40 (red), anti-actinin (green) antibodies, and DAPI (blue) nuclear staining. Panels D and E show *flox/flox*, and panels F and G show *flox/flox/cre*$^{+}$ littermate. Consistent with prior studies (Gourdie et al., 1993), Cx40 expression is absent in the proximal node (D and F) but is present in the His bundle (E and G). Expression of Cx40 is relatively preserved in Nkx2-5-deficient neonates, but overall, the AV node and His bundle appear smaller (arrows). (H–K) AChE activity stain of the AV node (H and J) and the His bundle (I and K), and counterstained with hematoxylin, in adult mice. The conduction system size as judged by AChE stain and overall morphology by hemotoxylin, or trichrome stain (not shown) is markedly atrophied in Nkx2-5-deficient mice.

mice. Using trichrome staining, we similarly observed selective degeneration of the central conduction system, as evidenced by selective cell dropout and fibrosis, while the surrounding atrial and ventricular myocardium is relatively preserved (Figure 3O). Similar analysis in mice heterozygous for the floxed allele (*flox/wt/cre*$^{+}$) showed no statistically significant change in the AV nodal size and, further, we were able to detect Nkx2-5

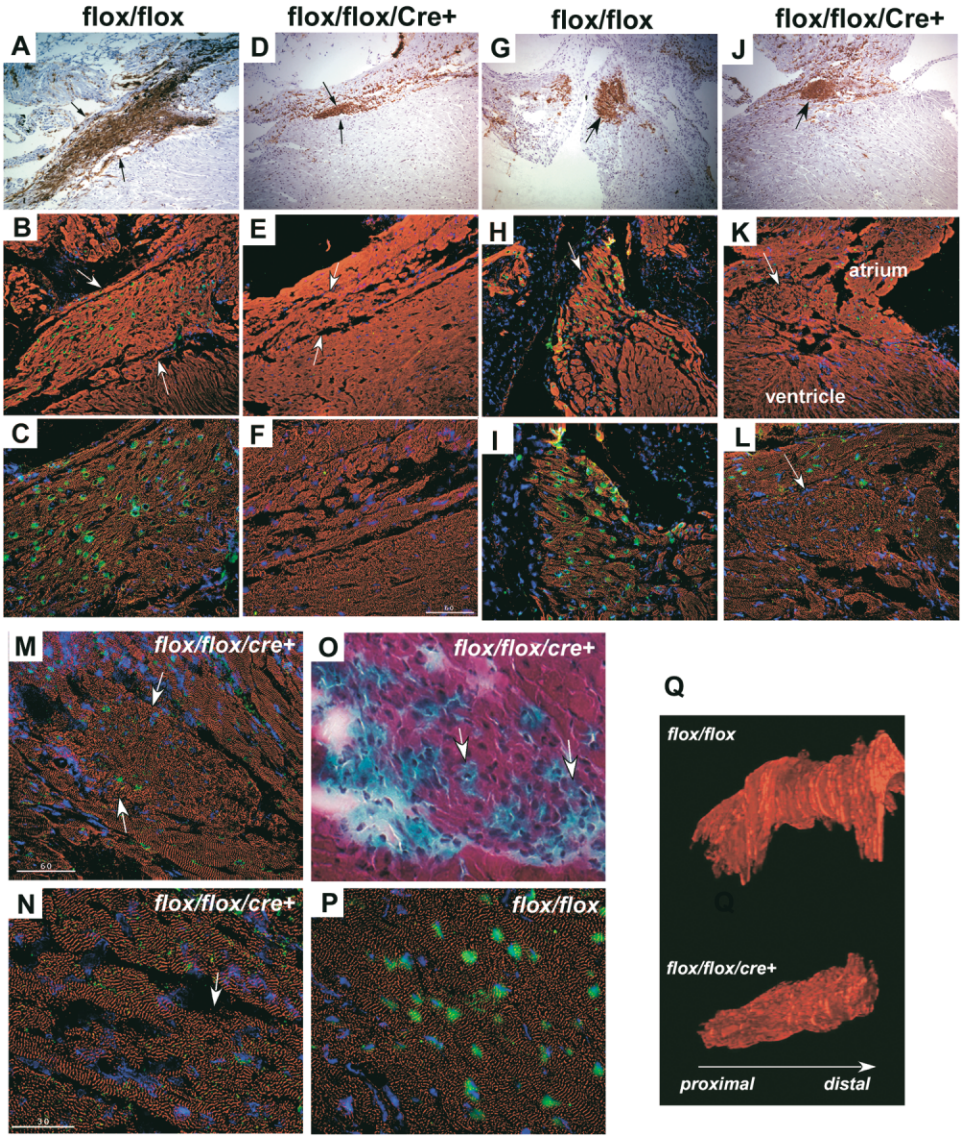

Figure 3. Comparison of the Central Conduction System in *flox/flox* and *flox/flox/cre*$^+$ Adult Mice

(A–L) Figure shows AChE and immunofluorescent staining of 12-week-old adult littermate hearts using anti-α-actinin (red) and anti-Nkx2-5 (green) antibodies. Cell nuclei were counterstained with DAPI (blue). Adjacent sections were stained with acetylcholinesterase to identify the AV node and His bundle (A, D, G, and J). In *flox/flox* (and wild-type, not shown) mice, the expression of Nkx2-5 as shown by the amount of immunoreactive protein is higher in the cells of the central conduction system compared to the surrounding working myocardium (B, C, H, and I). AV node (A to F) and the His bundle (G to L) are considerably smaller and atrophic in the *flox/flox/cre*$^+$ mice. There is little Nkx2-5 immunoreactive protein in the *flox/flox/cre*$^+$ mice, indicating high efficiency of cre recombination. At higher magnification (C, F, I, and L), marked loss of sarcomeric structure in the *flox/flox/cre*$^+$ conduction cells is evident (see Supplemental Figures online for larger high resolution images of the photomicrograph).

(M–N) Higher magnification views of the AV nodal cells in the adult *flox/flox/cre*$^+$ mice showing an atrophic AV node with cell loss and a disorganized sarcomeric structure (see Supplemental Figures online for larger high resolution images of the photomicrograph). Very few nuclei stained positive for Nkx2-5 in the *flox/flox/cre*$^+$ mice, but these cells had an overall healthier appearance with preserved sarcomeric structure.

(O) An adjacent section showing trichrome stain of the AV node showing marked fibrosis (arrows) and cell death.

(P) In contrast, the AV node in *flox/flox* mice shows robust cells with very organized sarcomeric structure. The expression of Nkx2-5 is higher in the cells of the conduction system.

(Q) Three-dimensional reconstruction of the AV nodes, showing a smaller and atrophic AV node in the *flox/flox/cre*$^+$ mice.

nuclear staining in virtually all cells (data not shown). To rule out the observed difference in size and morphology of the conduction system between the mouse populations as an artifact of sectioning, we generated a three-dimensional reconstruction of the AV node using the AChE positive areas from serial sections (Figure 3Q). As seen in the 3D reconstruction, there was a severe defect in the maturation and overall integrity of the AV node in the ventricular restricted *Nkx2-5* mutant mice. To determine whether there was a postnatal requirement for Nkx2-5 in the maintenance of AV nodal cells, sections containing AV node and His bundle were immunostained

for α-actinin as an additional parameter to allow for assessment of the integrity of conduction system myocytes. Using deconvolution microscopy (Agard et al., 1989), we systematically examined the sarcomeric integrity of the AV nodal cells. A clear striated pattern of organized sarcomeres was observed in the *flox/flox* conduction cells (Figure 3P). In contrast, conduction cells in the KO mice showed a dramatic sarcomeric and cellular disorganization (Figure 3N). Analysis of the AV node in *flox/flox/cre*$^+$ mice showed clear evidence of cell dropout and fibrosis in virtually all mice examined (Figure 3O). Therefore, the loss of a Nkx2-5-dependent pathway directly affected the integrity and sarcomeric structure of the conduction system myocytes. Our data show that the gradual process of AV block in mice with Nkx2-5 deficiency was primarily due to gradual nodal degeneration and cell dropout. Furthermore, this process appears to spare the surrounding myocardium, thus it is unlikely that AV nodal failure is due to cardiomyopathy (Figures 3D–3F).

Human Mutations in *Nkx2-5* Are Genetically Linked to Selective Myocyte Dropout/Fibrosis of the Distal AV Node and Cardiomyopathy

We re-analyzed the electrophysiological data of a large Oregon kindred affected by a mutation in *Nkx2-5* (Gln198ter, MBX family) that produced a truncated protein that lacks a portion of the 3′ coding region (Schott et al., 1998). This family displayed a high penetrance of advanced AV conduction block, and clinical electrophysiological studies have revealed a marked dysfunction of the AV node and His bundle. In several individuals with mutations of *Nkx2-5*, the advanced nature of the conduction block eventually necessitated pacemaker implantation, with incidents of unexpected death, likely due to malignant cardiac arrhythmias. In two individuals, autopsy specimens became available, thereby allowing for a rigorous, direct analysis of the conduction system in the hearts of patients heterozygous for this *Nkx2-5* mutation. As shown in Figures 4A–4F, this human mutation in *Nkx2-5* was associated with a marked, preferential degeneration of the conduction system at the level of AV node and the His bundle, while the surrounding myocardium is relatively unaffected. In both cases, only remnants of conduction cells were identifiable at the anatomical location of the AV node and His bundle, which was noted by prominent AV nodal myocyte dropout and fatty replacement. Similar histological analyses in a large series of human autopsy specimens revealed the selective AV nodal degeneration to be unique (Anderson and Ho, 2001). Thus, human mutations in *Nkx2-5* are genetically linked with selective myocyte dropout and fibrosis of the AV node, and progressive heart block, supporting the pivotal, selective role of Nkx2-5 signals for the maintenance and maturation of human AV nodal myocytes. In addition, histological analysis of these patient specimens also revealed evidence of hypertrophic cardiomyopathy.

Nkx2-5-Deficient Hearts Show a Novel Form of Perinatal and Adult Cardiomyopathy

Examination of newborn mutant hearts showed marked cardiac enlargement with trabeculae that filled the left ventricular cavity (Figure 5A). A prominent feature of cardiomyopathy in neonatal mice was extensive trabeculae and evidence of myocardial noncompaction. Immunostaining analysis of the neonatal ventricle with an anti α-actinin antibody (Figure 5A, middle panel) confirmed that long trabecular projections were indeed cardiomyocytes. Assays for postnatal myocardial growth by anti-phospho-histone H3 immunostaining in the ventricular myocytes revealed a significantly higher number of cells ($p < 0.02$) per section that stained positive for phospho-histone H3 (Figure 5A, bottom panel). Progression to heart failure with concomitant dilatation of both chambers and more prominent trabeculae was evident with 100% penetrance in adult mice (Figure 5D). Echocardiographic evaluation of the mutant hearts and their littermates confirmed the presence of cardiomyopathy with increased septal ($n = 11$, $p < 0.01$) and posterior wall ($p < 0.02$) thickness, and a mild reduction in left ventricular function ($p < 0.02$) at 14 weeks postgestation (Figure 5C). Echocardiographic examination also revealed the presence of prominent trabecular formations and evidence of noncompaction in both ventricular chambers. The echocardiographic and histologic evidence of hypertrabeculation and noncompaction in *Nkx2-5* mutant mice is consistent with the echocardiographic and histological criteria for ventricular noncompaction in man (Jenni et al., 2001). Prior studies have also shown ventricular noncompaction in a patient with a chromosomal deletion of the *Nkx2-5* locus (Pauli et al., 1999).

Dysregulation of Downstream Target Genes in *Nkx2-5* Mutant Hearts

In an effort to identify molecular pathways involved in AV nodal block and the hypertrabeculation in adult Nkx2-5-deficient mice, we compared the gene expression profiles of *flox/flox* and *flox/flox/cre*$^+$ hearts by microarray analysis. Pooled ventricular RNA was isolated from three mice in each group and was used for microarray analysis; each experiment was repeated three times. Using strict selection criteria for signal strength, expression ratio, background, and reproducibility, several genes showed a dramatic (5-fold or higher) change in the level of expression. Genes associated with myocardial cell proliferation and trabeculation were markedly dysregulated in the mutant hearts, including bone morphogenic protein-10 (BMP-10), which is aberrantly expressed at high levels in the KO ventricle, and the cardiac homeodomain-only protein, HOP, which was downregulated 5-fold. BMP-10 is a key regulator of cardiac morphogenesis and myocardial trabecular formation (Neuhaus et al., 1999). Mice with a targeted disruption of BMP-10 die in mid-gestation due to heart failure and by histology they have a thinned, poorly developed myocardium (Chen et al., 2004). HOP is a homeodomain-only protein that is a downstream target of Nkx2-5 (Chen et al., 2002; Shin et al., 2002). A targeted disruption of HOP resulted in postnatal myocardial overgrowth and hyperplasia in a subset of KO progeny (Shin et al., 2002). In addition, two ion channels that are normally predominantly expressed in the conduction system were specifically affected by Nkx2-5 deficiency in the mutant hearts. The expression of a pacemaker channel, i.e., the hyperpo-

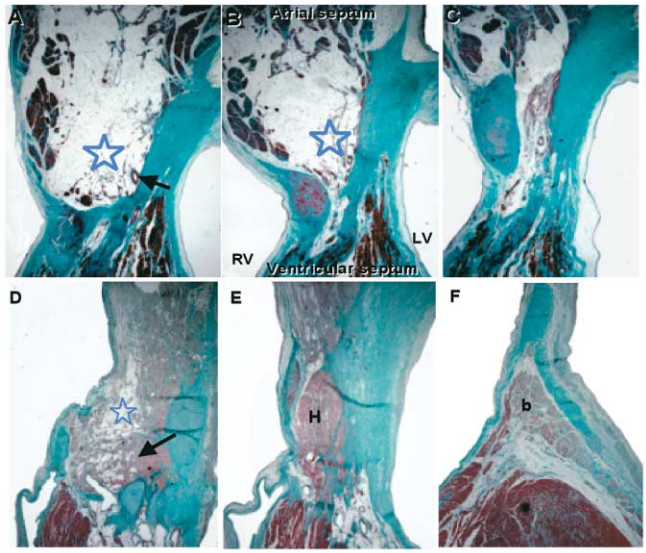

Figure 4. Conduction System Disease in a Patient with Mutation of *Nkx2-5* Gene

Sections of post-mortem heart from a patient with *Nkx2-5* mutation were analyzed by trichrome stain (myocardium in red; fibrous tissue in green).

(A) Star marks the anticipated area of the AV node that is occupied by fatty tissue with residual strands of compact nodal cells close to the nodal artery (arrow). Transitional cells are absent.

(B) This section taken superiorly to section A shows the anticipated region of the nodal-His bundle junction (star). Only a few strands of conduction tissues remain.

(C) This section shows the most substantial portion of the His bundle passing through the central fibrous body. Again, there is fatty and fibrous replacement evident.

(D) There is a remnant of the compact AV node (arrow) but the zone of transitional cells and right part of the node are largely replaced by fatty tissue (star).

(E) and (F) show His bundle (*H*) and branching bundles (*b*).

(G) Cross-sections of a normal heart and heart from a patient with *Nkx2-5* mutation who died unexpectedly. Compared to the control, *Nkx2-5* mutant heart has marked left ventricular hypertrophy and more prominent ventricular trabeculae.

larization-activated cyclic nucleotide-gated channel, HCN-1, was markedly and aberrantly elevated in the mutant hearts (>20-fold by quantitative RT-PCR, not shown), while the minimal potassium channel (minK, KCNE-1) was downregulated (5-fold) in the ventricle (Figure 6A, quantitative data not shown). An atrial-restricted inhibitor of the sarcoplasmic reticulum calcium ATPase, sarcolipin (Minamisawa et al., 2003), was markedly upregulated and aberrantly expressed in the ventricle (>50-fold). Other markers of fetal gene expression, including ANF, BNP, and β-MHC, showed only modest increases (1.5- to 2-fold), suggesting that the cardiomyopathy associated with the loss of Nkx2-5 signals is distinct from common forms of hypertrophic cardiomyopathy. Other genes such as MLC2v, troponin I, and myosin binding protein-C showed only a 1.2- to 1.4-fold decrease in gene expression. We confirmed the expression profiles of these selected genes by RT-PCR (Figure 6A), quantitative RT-PCR (not shown), and Northern blot analysis (not shown), which was further corroborated by expression microarray analysis. Bioinformatic analysis of 156 publicly available databases (http://cardiogenesis.med.harvard.edu/home) revealed the upregulation of BMP-10, sarcolipin, and HCN-1 to be unique to the cardiomyopathy associated with Nkx2-5 defects (see Supplemental Data online for further details).

Altered Gene Expression in the Conduction System

In ventricular myocardium, connexin 40 (Cx40) is restricted to the distal AV node and the His-Purkinje system (Gourdie et al., 1993). Furthermore, Cx40 is a downstream target of TBX5 and Nkx2-5 (Bruneau et al., 2001) and there are NKE binding sites within the mouse Cx40 promoter. While present in the neonatal *flox/flox/cre*$^{+}$ mice (Figure 2, D-G), Cx40 is virtually absent in the adult mutant conduction system (Figure 6, B-E). These data are consistent with Nkx2-5 being a positive regulator of Cx40 gene expression (Bruneau et al., 2001) and further suggest a specific role for Nkx2-5 in the postnatal conduction system maturation and maintenance.

More recently, a minK-lacZ (minimal potassium channel, KCNE-1) mouse line has been utilized to track the development and maturation of the mouse conduction system cells (Kondo et al., 2003; Kupershmidt et al., 1999; Nguyen-Tran et al., 2000). Since RT-PCR and microarray analysis suggested that minK is a potential downstream target for Nkx2-5, we crossed the minK-lacZ knockin mouse into the mouse line with *Nkx2-5* haplo-insufficiency and generated double heterozygotes. As shown in Figure 6 (panels F-I), the degree of lacZ staining is significantly lower in mice heterozygous for *Nkx2-5*, suggesting an Nkx2-5 dependent gene dosage affect. Immunostaining of the *flox/flox/cre*$^{+}$ ventri-

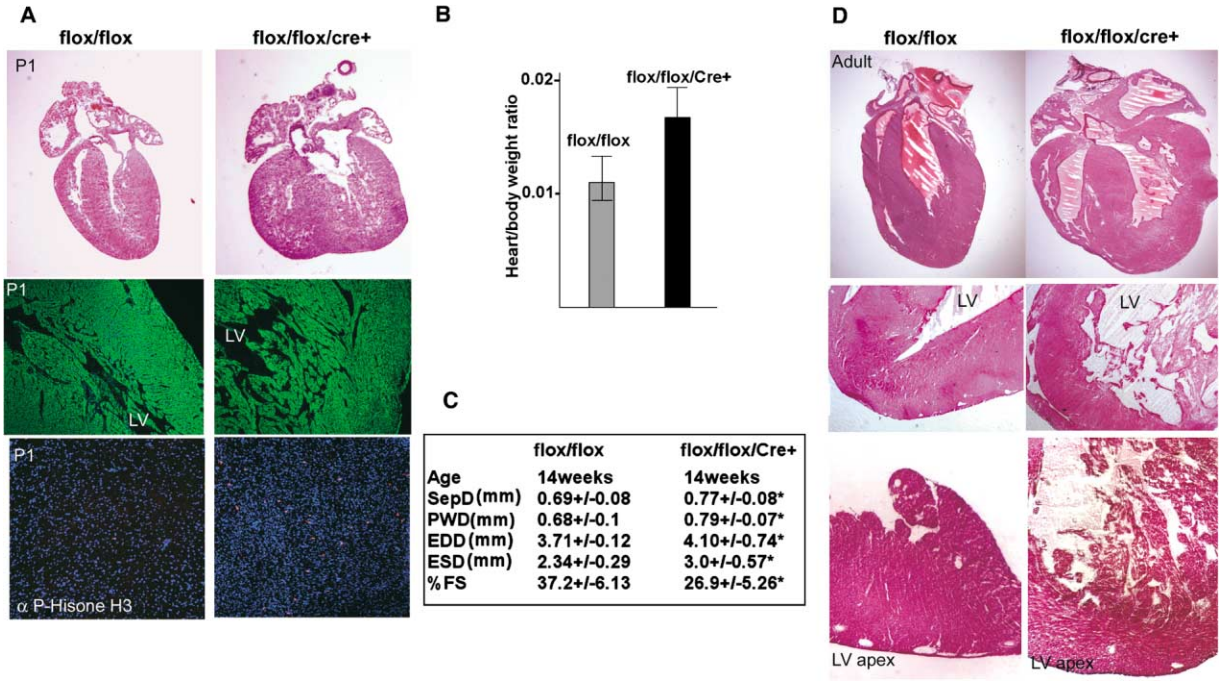

	flox/flox	flox/flox/Cre+
Age	14weeks	14weeks
SepD(mm)	0.69+/-0.08	0.77+/-0.08*
PWD(mm)	0.68+/-0.1	0.79+/-0.07*
EDD(mm)	3.71+/-0.12	4.10+/-0.74*
ESD(mm)	2.34+/-0.29	3.0+/-0.57*
%FS	37.2+/-6.13	26.9+/-5.26*

Figure 5. Cardiomyopathy in Nkx2-5-Deficient Mice

(A) Top panel, postnatal day 1 (P1) *flox/flox* (left) and *flox/flox/cre*$^+$ (right) isolated hearts showing marked cardiac enlargement at birth in Nkx2-5-deficient heart. Middle panels show α-actinin (green) immunostaining in the neonatal left ventricle showing marked trabeculae in the LV cavity of *flox/flox/cre*$^+$ mice. Lower panels show immunostaining with anti-phospho-histone H3 (red) and nuclear stain DAPI (blue). The neonatal *flox/flox/cre*$^+$ hearts show a marked increase in cellular mitosis as evidenced by an increase in phospho-histone H3 immunoreactivity.

(B) Heart to body weight ratio of adult (average 14 weeks) hearts ($n = 7$; $p < 0.005$).

(C) Echocardiographic parameters in adult *flox/flox* and *flox/flox/cre*$^+$ mice.

(D) Cardiomyopathy in adult (30 weeks) *flox/flox/cre*$^+$ mouse compared to its *flox/flox* littermates (*flox/flox* on left, *flox/flox/cre*$^+$ on right). Virtually all adult mutants showed a severe form of cardiomyopathy (H & E stain). Note the hypertrophied heart and extensive trabeculae in the mutant (middle panel). Bottom panels show the extensive trabeculae in 42-week-old *flox/flox/cre*$^+$ mice. In addition, compared to the *flox/flox* heart, the Nkx2-5-deficient heart shows histologic evidence of noncompaction.

cles with anti-minK antibodies failed to detect an appreciable signal (data not shown).

The hyperpolarization-activated cation current plays a key role in the initiation and modulation of the depolarization of cardiac pacemaker cell lineages. Recently, the hyperpolarization cyclic nucleotide gated (HCN) family has been identified as the molecular correlates of the pacemaker cation current (Biel et al., 2002). The HCN channels 1, 2, and 4 are expressed in the heart; among these, HCN 1 and 4 are primarily expressed in the SA node, while HCN 2 is also expressed in the ventricle (Azene et al., 2003; Han et al., 2002). Our studies have now shown that HCN-1 is expressed in the conduction system including the SA node (not shown), AV node (Figures 6J and 6L), and His-Purkinje cells (not shown). HCN-1 is aberrantly expressed in the ventricle of Nkx2-5 deficient mice (Figure 6M), while the spatial expression of the HCN4 gene was relatively unaffected. These findings were confirmed by quantitative RT-PCR and expression microarray analysis (data not shown). In sum, our findings document the dysregulation of markers (atrial, conduction system, and trabecular) for the identity of distinct cardiac muscle cell lineages, indicating a fundamental defect in ventricular cell lineage maturation and specification in the absence of Nkx2-5.

Overexpression of BMP-10 Leads to Myocardial Overgrowth and Hypertrabeculation

Microarray analysis of ventricular RNA and real-time RT-PCR (not shown) confirmed marked aberrant expression of BMP-10 in Nkx2-5-deficient neonates and adults. Since BMP-10 is expressed in mice during a critical window of embryonic ventricular development (i.e., ED 9.0 to ED 15.5), we sought to determine the role of BMP-10 overexpression in the onset of the cardiac muscle cell phenotype in the ventricular restricted Nkx2-5 KO mice. BMP-10, a member of the TGF-β family, is a cardiac restricted factor that is predominantly expressed in the trabeculae of the developing heart (Neuhaus et al., 1999). BMP-10 expression is first noted during ED 9.0 in the ventricle during the onset of the formation of the trabecular layer of the fetal ventricular chamber and, later at ED 12.5 expression, is noted in the atria. However, at mid-gestation (ED 15.5–16.5) and after formation of the trabecular network, BMP-10 mRNA is no longer detectable in the ventricle and localizes only to the atria (Chen et al., 2004; Figure 7A). In the adult mouse ventricle, BMP-10 is undetectable by in situ hybridization (Figure 7B, left panel). In contrast, in the ventricular restricted Nkx2-5 KO, we observed persistent, marked expression of BMP-10 predominantly in the trabeculae

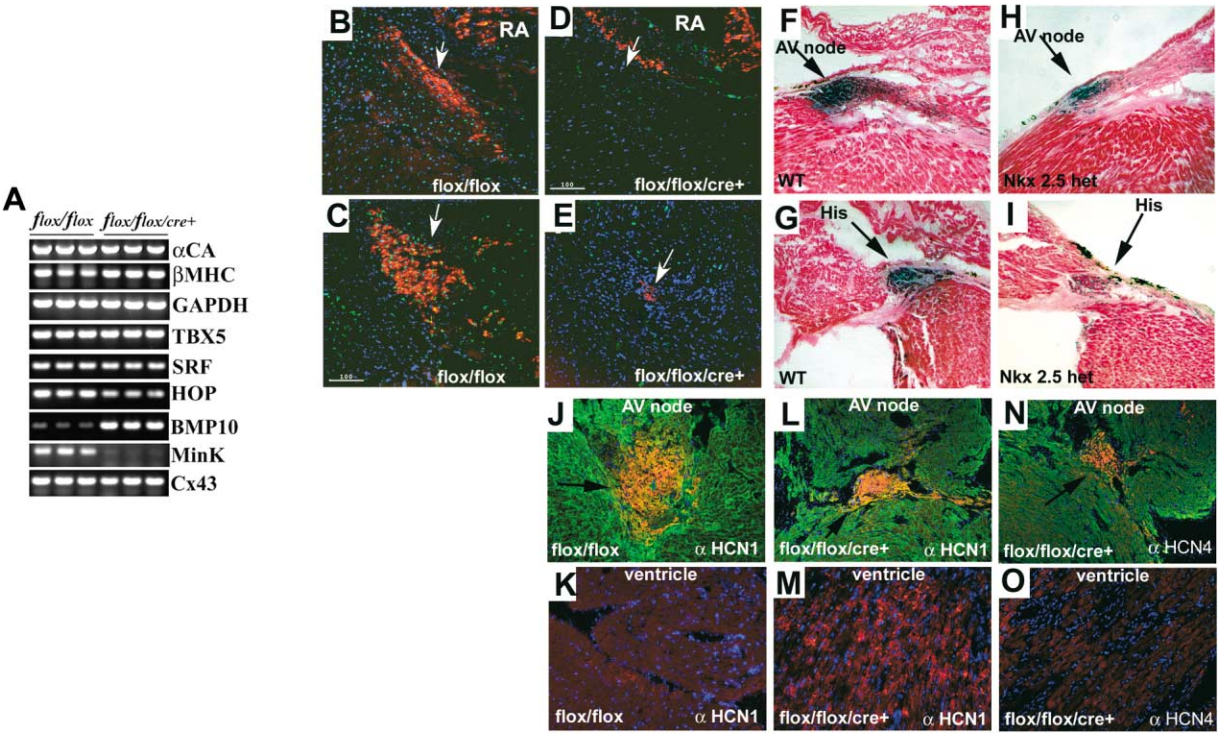

Figure 6. Altered Gene Expression in the Conduction System of Nkx2-5-Deficient Mice

(A) RT-PCR analysis of adult (10–12 weeks) ventricular RNA from *flox/flox* and *flox/flox/cre*$^+$ littermates shows selected genes that show altered or relatively unchanged expression pattern. αCA = α cardiac actin; Cx43 = connexin 43; SRF: serum response factor; BMP-10 = bone morphogenic protein-10; mink = minimal potassium channel (KCNE-1).

(B–E) Immunostaining of *flox/flox* (panels B and C) and *flox/flox/cre*$^+$ (D and E) heart sections using anti-Cx40 antibody (red), anti-Nkx2-5 antibody (green), and DAPI (blue). Cx40 (white arrows) expression is present in the adult *flox/flox* distal AV node (B) and His bundle (C) and the right atrium (RA). Cx40 is virtually absent in the respective sections (D and E) from *flox/flox/cre*$^+$ littermates.

(F–I) LacZ stain of the AV node (F, black arrows) and the His bundle (G) in mice with minK lacZ-knockin (Kupershmidt, et al., 1999; Kondo et al., 2003). (H–I) The AV node (H) and His bundle (I) in mice heterozygous for *Nkx2-5* and minK lacZ-knockin show a markedly diminished lacZ staining consistent with *Nkx2-5* gene dosage effect on minK expression.

(J–O) Immunostaining of the *flox/flox* (J and K) and *flox/flox/cre*$^+$ (L and M) mice heart sections using anti-HCN-1 (J–M) and anti-HCN-4 (N and O) antibodies. Within heart, both HCN-1 (red) and HCN-4 (red) are predominantly expressed in the conduction system (black arrows, panels J, L, and N) (for review, see Biel et al., 2002). Cardiomyocytes are labeled with anti-α-actinin (green) and nuclei are labeled blue with DAPI. In the ventricle (K, M, and O), the HCN-1 is aberrantly expressed in the *flox/flox/cre*$^+$ ventricle.

of virtually all adult *flox/flox/cre*$^+$ mice (Figure 7B, right panel). Given the extensive trabecular formations noted in both ventricles, overexpression of BMP-10 might positively modulate myocardial overgrowth and hypertrabeculation. To further confirm the myocardial growth in adult mice, we assayed for phospho-histone H3, a marker of mitosis, by immunostaining (Figure 5A, bottom panels) in neonatal as well as adult hearts (data for adult heart similar to neonatal heart, not shown). Cardiac muscle cells normally begin to withdraw from the cell cycle at birth. However, in Nkx2-5-deficient hearts, we see evidence for persistent cellular mitosis at the neonatal stage extending into adult life. The fact that cells staining positive for phospho-histone H3 also stain positive for sarcomeric α-actinin (data not shown) indicates that the cells undergoing mitosis are myocytes. To determine if BMP-10 can positively regulate myocardial growth, we assayed for the rate of DNA synthesis (thymidine incorporation) in embryonic cardiomyocytes in the presence of BMP-10 (Figure 7D). Embryonic cardiomyocytes from ED 13.5 wild-type mice were incubated with conditioned media containing secreted BMP-10 or control media. In vitro experiments revealed an increase in cell growth, as evidenced by increased DNA synthesis in embryonic cardiomyocytes ($p < 0.001$; Chen et al., 2004). We also observed that the rate of thymidine incorporation in the cardiomyocytes from BMP-10 KO embryos was markedly reduced, thereby indicating that BMP-10 was required for the proper growth and/or differentiation of at least a subset of cardiomyocytes (Figure 7E). In a transgenic mouse model where the expression of BMP-10 was anomalously elevated via ANF promoter, there was a similar pattern of myocardial overgrowth and hypertrabeculation (Figure 7C). In line with these observations, mouse embryos lacking BMP-10 showed a hypoplastic heart with thinning of the septum and the ventricular wall and died in early gestation (ED 10.5) (Chen et al., 2004). In addition, BMP-10 KO embryos were found to have a normal level of Nkx2-5 expression in the myocardium at ED 8.5–8.75; but this was dramatically downregulated at ED 9.25–9.5, shortly after BMP-10 expression is normally initiated in the embry-

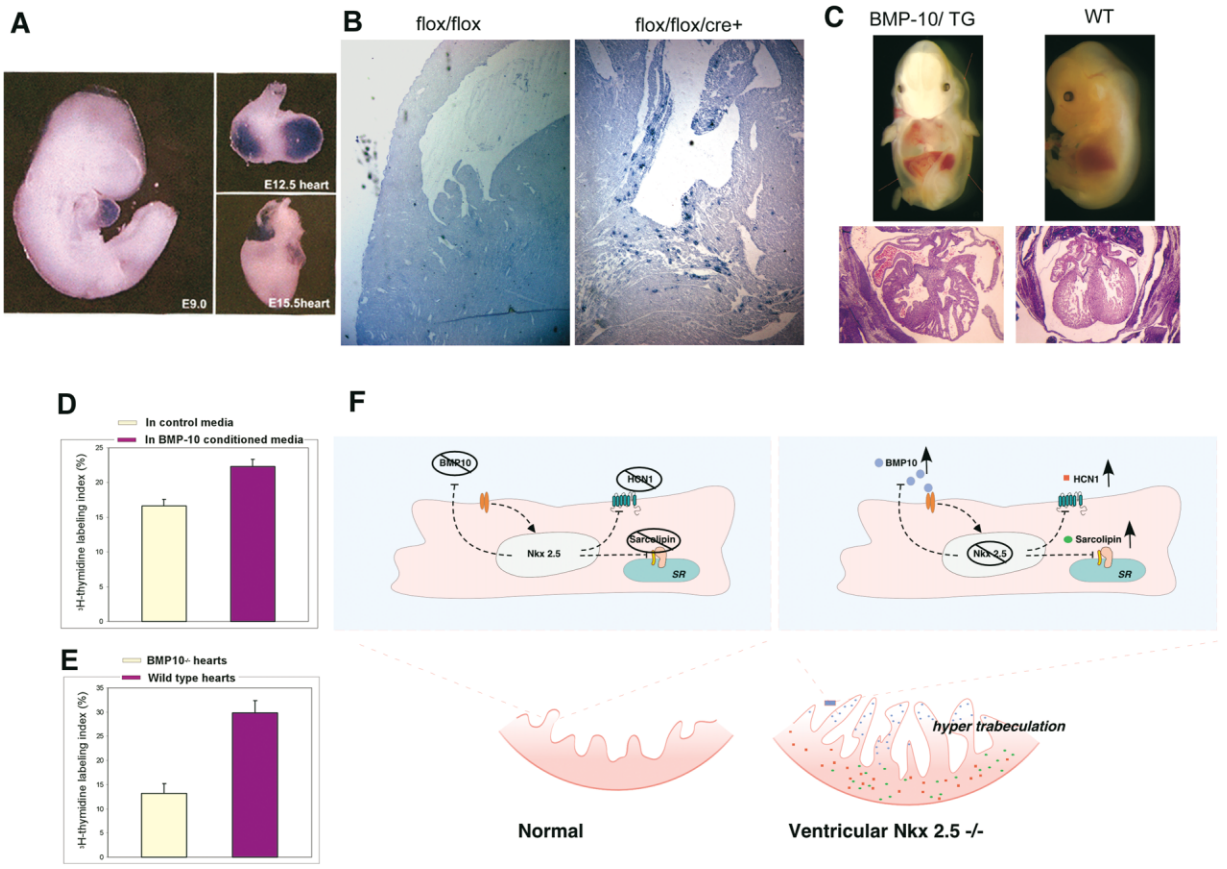

Figure 7. Overexpression of BMP-10 in the Nkx2-5-Deficient Hearts

(A) In situ hybridization using antisense BMP-10 mRNA in wild-type embryonic heart. BMP-10 is first detected around ED 9, and at ED 12.5, it is restricted to the trabecular myocardium. At ED 15.5, BMP-10 is absent in the ventricule and is only expressed in the atria.

(B) In situ hybridization using antisense BMP-10 probes in the adult mice showing intense trabecular staining in the *flox/flox/cre*$^{+}$ hearts. There is no detectable BMP-10 expression in the *flox/flox* ventricle.

(C) Overexpression of BMP-10 in developing hearts leads to overproduction of ventricular trabeculae and abnormal formation of ventricular septum (Chen et al., 2004). Left panels show ANF-BMP-10 transgene positive embryos (E14.5). Lower panels represent the histological sections of WT and BMP-10-overexpressing transgenic mice (BMP-10/TG).

(D) Embryonic cardiomyocytes (ED 13.5) were cultured in BMP-10 conditioned or control media. ^{3}H-thymidine labeling index is significantly higher in cardiomyocytes cultured in BMP-10 conditioned media after 48 hr of culture ($p < 0.05$).

(E) BMP-10-deficient hearts have dramatically reduced ^{3}H-thymidine labeling index when compared to littermate controls ($p < 0.001$).

(F) An illustration summarizing the molecular pathways and the phenotypic consequences observed in our studies as a result of Nkx2-5 depletion in ventricular myocytes. In the control ventricular myocytes (left panel), Nkx2-5 is normally expressed and as a result, BMP-10, HCN1, and sarcolipin expression are suppressed in adult ventricular myocytes. In the absence of Nkx2-5 (right panel), there is aberrant expression of BMP-10 at the trabeculae throughout the postnatal period into adulthood, driving the observed phenotype of hypertrabeculation. Sarcolipin (normally atrial restricted) and HCN1 (normally conduction system restricted) both have significantly elevated expression in adult ventricular myocytes in the absence of Nkx2-5, indicating a defect in lineage specification and maturation.

onic heart (Chen et al., 2004). These data suggest that BMP-10 and Nkx2-5 can coordinately modulate embryonic myocardial growth and development. The fact that BMP-10 expression was aberrantly increased in Nkx2-5 ventricular restricted KO mice suggests that Nkx2-5 is a negative regulator of BMP-10 expression. A recent study provides further direct evidence that Nkx2-5 and BMP-10 modulate the growth and differentiation of ventricular myocardium (Chen et al., 2004). Taken together, the gain- and loss-of-function studies of BMP-10 in both in vitro and vivo model systems supported the role of a novel pathway for ventricular muscle cell lineage growth that is mediated by a Nkx2-5-BMP-10 axis (Figure 7F). Dysregulation of this axis can directly account for an important subset of the ventricular muscle phenotype seen in the setting of *Nkx2-5* mutations.

Discussion

Nkx2-5 Pathways and Ventricular Lineage Specification

The present study employs a conditional mutagenesis strategy to define the potential role of Nkx2-5 within cardiac myocyte lineages at later stages of heart development. Interestingly, these mice display many of the ventricular muscle cell phenotypes seen in the hearts of patients who harbor mutations in Nkx2-5, including cardiomyopathy, and progressive postnatal AV block,

but without evidence of congenital heart disease, i.e., atrial or ventricular septal defects. A detailed, comprehensive analysis of the downstream target genes that are disrupted in these mutant mice, based on a combination of bioinformatics and microarray analysis of ventricular gene expression, reveals a defect in ventricular lineage specification, as evidenced by the aberrant expression of atrial, conduction system, and trabecular restricted markers within the working myocardium of the postnatal hearts. As such, these studies identify a new molecular paradigm for the onset of congenital heart defects and associated arrhythmogenesis via defects in the decision-making steps that guide ventricular cells into discrete cardiomyocyte lineages. Since the ectopic ventricular expression of several of these genes is persistent and their effects are now known to directly influence automaticity (HCN1), contractility (sarcolipin), and trabeculation (BMP-10), these studies support the concept that the surgical correction of the structural morphogenic heart defects is unlikely to correct the underlying molecular defects, thereby leading to progressive dysfunction in the postnatal heart in discrete cardiac muscle cell lineages.

Ventricular Nkx2-5 Pathways for AV Nodal Myocytes Lineage Formation and Maturation: Relationship to Arrhythmogenesis

By analysis of AV nodal cardiac myocyte lineages in the ventricular restricted *Nkx2-5* mutant mice, the present study documents that Nkx2-5-dependent pathways within ventricular lineages play a critical role in the maturation and maintenance of AV nodal myocyte lineages. At birth, hypoplasia of the AV node is evident in the ventricular restricted *Nkx2-5* mutant mice, with the node displaying a 50% decrease in size when compared to the wild-type. The data in the present study now identify Nkx2-5 as an intrinsic pathway within ventricular myocyte lineages that is most likely required in combination with the extrinsic cues to drive formation of the AV nodal lineages within the central conduction system.

Herein, we present evidence supporting a plausible molecular mechanism leading to progressive complete heart block. Many arrhythmias are believed to be congenital (Long QT and WPW) even if first discovered later in life, but many more are believed to be acquired and result from ischemic (ventricular tachycardia, AV block) or other degenerative (AV block, bundle branch block) processes. The discovery of discrete genetic pathways leading to premature AV nodal degeneration and conduction abnormalities suggests that "acquired" arrhythmias may also be in part "congenital" in nature. Taken together, the current study provides evidence for a two-hit model for the onset of progressive heart block and AV nodal dysfunction that occurs due to the loss of cell-autonomous Nkx2-5 pathways. The first hit consists of a smaller AV node that reflects a critical role of Nkx2-5 in the initial formation of AV nodal myocytes from ventricular progenitors. At birth, this hypoplastic AV node is capable of maintaining AV nodal function, at a time when the atrial and ventricular chambers and the distal conduction system are not yet fully developed. The second hit may be the stimulus of stress-induced signals leading to normal postnatal cardiac growth and maturation in the presence of Nkx2-5; In the absence of Nkx2-5, the same signals may ultimately lead to AV nodal myocyte degeneration and complete heart block.

BMP-10 Pathways and Ventricular Muscle Cell Lineage Defects

One of the most critical steps of ventricular chamber development is the formation of a finger-like meshwork of myocardial cells known as trabecular myocardial layer in the fetal heart. The process of trabeculation is critically linked with the control of cardiac muscle growth, as the rapid burst in the expansion of the trabecular myocardium is normally followed by subsequent differentiation and slower cycling rate of the cells at the outermost boundary of the trabecular myocardium; these cells differentiate into conduction system lineages known as Purkinje fibers (Sedmera et al., 2003). Cardiac muscle cells normally begin to withdraw from the cell cycle at birth. In this manner, the precise control of trabecular muscle growth may play a critical role in the onset of many aspects of congenital heart disease phenotypes, i.e., trabeculation, septation, and conduction, seen in the setting of *Nkx2-5* mutations in both experimental models and in patients. Accordingly, understanding the molecular mechanisms responsible for the onset of defects in ventricular maturation and myocyte differentiation are central to unraveling the logic of many forms of congenital heart disease. In a recently described model, mice deficient for the transcription factor HOP, a downstream target for Nkx2-5, showed persistent cell growth and hyperplasia in the immediate postnatal stage, but not in the adult animals (Shin et al., 2002). Similarly, mice deficient for Nkx2-5 show a markedly lower level of HOP expression with a similar evidence of myocyte hyperplasia and postnatal growth. Surprisingly, in this instance, we find persistence of trabecular growth into adult life.

In the present study, we have now identified a dysregulation of the Nkx2-5-BMP-10 axis as a critical step in the onset of this trabecular defect. The ventricular restricted *Nkx2-5* mutant mouse hearts display prominent hypertrabeculation and cardiomyopathy. Using this mouse model, we have shown that there is aberrant postnatal expression of BMP-10, which is normally expressed in ventricular myocardium during the initial stages of trabeculation (Neuhaus et al., 1999). After ED 15.5, BMP-10 expression is completely extinguished in the ventricular myocardium, coinciding with the period of trabeculae and compact zone expansion. This temporal association implicated BMP-10 in the hypertrabeculation in the *Nkx2-5* mutant hearts. Three independent approaches support this contention, i.e., a direct effect of BMP-10 on promoting ventricular cell proliferation in vitro, a marked increase in ventricular muscle cell proliferation in vivo in transgenic mice that overexpress BMP-10 in the myocardium, and BMP-10 KO mice that display a complete loss of ventricular chamber proliferation. Taken together, these studies point to the persistent expression of BMP-10 as playing a critical role in the onset and progression of defects in ventricular muscle cell lineages in the *Nkx2-5* mutant hearts and suggest that this persistent expression of a known ventricular growth factor may partially account for the ventricular defects seen in the *Nkx2-5* mutant mice. Since other

factors that regulate ventricular trabeculation, such as neuregulin, have already been implicated in the onset of conduction system lineage formation (Gassmann et al., 1995; Lee et al., 1995; Rentschler et al., 2002), BMP-10 might also play a dual role in regulating the formation of conduction system lineages during cardiac chamber maturation. These studies support the notion that an Nkx2-5-BMP-10 axis plays a critical role in ventricular muscle cell lineage specification and provide a working model for a molecular pathway for the onset of multiple ventricular defects in an important form of human congenital heart disease (Figure 7F). It will become of interest to determine if antagonism of chronic BMP-10 signals may represent a new therapeutic approach to prevent progressive cardiac defects in genetic forms of human congenital heart disease.

Experimental Procedures

Generation of Nkx2-5 Ventricular Restricted KO Mouse

The *Nkx2-5 floxed* allele was generated using a previously described strategy (see Supplemental Data on *Cell* website for details; Chen et al., 1998). Two independent targeted ES cell clones were introduced into C57/B6 mouse blastocysts as described (Nagy et al., 1990). Mice homozygous for *floxed Nkx2-5* allele were crossed into MLC2v-cre (Chen et al., 1998) background to generate ventricular KO of Nkx2-5. All mice used in this study are derived from 129/sv crossed into either Black Swiss or C57/B6 background. Genotyping was performed by PCR analysis of tail DNA using *Cre*-specific primers and primers that spanned intron 1 and exon 2 of *Nkx2-5* gene.

Telemetry and Surface ECG

Methods were performed as described previously (Nguyen-Tran et al., 2000). For details, see online Supplemental Data.

Histological Analyses

Unless otherwise mentioned, cryosections were used. Freshly harvested mouse hearts were embedded in OTC freezing media and snap frozen using 5-methylbutane (Sigma) and liquid nitrogen. Hearts were allowed to freeze overnight in −80°C freezer stored in airtight container. Prior to sectioning, the OTC embedded block is equilibrated in −20°C for at least 15 min. Five to ten micron sections were collected onto Superfrost Plus glass slides (Fisher Scientific). For serial sections through the AV node, anatomical landmarks were used to help guide the decision to begin collection. Two sections were placed on each glass slide and any loss of sections was noted. Acetylcholinesterase staining was performed based on protocols developed previously (El-Badawi and Schenk, 1967).

Immunohistochemistry and Imaging

Five micron frozen sections were collected on glass slides and fixed in cold (−20°C) 100% methanol for 1 min. Sections were then incubated in PBS containing 1% BSA, 0.3% Triton X-100 for 15 min. Antibodies were used at 1:500–1:100 dilutions in PBS/1%BSA overnight at 4°C. The slides were then washed in solutions containing PBS/1%BSA for 20 min and then incubated with secondary antibody (1:100 dilution) for 1 hr at room temperature. The primary antibodies included anti-Nkx2-5 (Santa Cruz Biotechnology, Santa Cruz, California), anti-sarcomeric α-actin monoclonal (Sigma), and anti-connexin 40 (Chemicon, California), and anti-phospho-Histone-H3 (Upstate, Waltham, Massachusetts) antibodies. The secondary antibodies were purchased from Molecular Probes (Eugene, Oregon) and Jackson ImmunoResearch (West Grove, Pennsylvania). Images were captured by deconvolution microscopy (Agard et al., 1989) using a DeltaVision deconvolution microscopic system operated by SoftWorx software (Applied Precision). Pixel intensities were kept in the linear response range of the digital camera. Optical sections through the samples were taken with increments of 0.2–0.5 μm depending on magnification. The images were deconvolved and examined either section by section or volume views were generated by combining areas of maximal intensity of each optical section with SoftWorx programs. Data Inspector application was used to quantitatively analyze the images. Adobe Photoshop 6.0 was used to design figures.

Human Histology

Postmortem examination of the human cardiac conduction system was performed as described previously (Ho and Anderson, 2000).

In Situ Hybridization

Full-length BMP-10 cDNA (gift from Vicki Rosen) was linearized with BamHI. Nonradioactive antisense RNA probe was generated using T7 RNA polymerase. Whole-mount in situ hybridization was performed as previously described (St Amand et al., 2000).

3D Reconstruction of the AVN

For details, see Supplemental Data on *Cell* website.

RNA Isolation and Quantitative RT-PCR Analysis

Total RNA was isolated from microdissected ventricles. Ventricular tissue was either homogenized in Trizol reagent (Gibco BRL) to isolate total RNA or isolated using RNeasy Mini Kit by following manufacturer's protocols (Qiagen). Quantitative RT-PCR was performed using Qiagen's QuantiTect SYBR RT-PCR kit and transcript-specific primers. Stratagene's MX400 PCR machine was used for real-time detection of fluorescent signal emitted by amplicons. Each reaction contained 100–200 ng of total RNA and the relative quantity between two samples were calculated utilizing the ΔΔCt method, normalizing to either GAPDH or β-actin Ct (threshold cycles) (Livak and Schmittgen, 2001).

Microarray Data Analysis

For details, see online Supplemental Data.

Histological, Morphological, and ^{3}H-Thymidine Labeling Index Analyses

Embryos and isolated hearts were fixed in 10% neutral buffered formalin, paraffin embedded, and sectioned (6 μm), and stained with hematoxylin and eosin. To analyze the proliferative activity of developing heart, timing-mated females were given a single injection of tritiated thymidine (200 μCi ip at 28 Ci/mM; Amersham Biosciences Corp.). Embryos were harvested after a 4 hr labeling period and followed by fixation (10% neutral buffered formalin) and paraffin section. Deparaffined sections were stained with Hoechst in PBS to illustrate nucleus. The Hoechst-stained slides were coated with photographic emulsion (Polysciences, Inc., Warrington, Pennsylvania) and further processed for autoradiography. ^{3}H-thymidine labeling index was the percent of total number of labeled nucleus versus total number of nucleus.

Generation of BMP-10-Expressing NIH3T3 Cells and Culture of Embryonic Cardiomyocytes using BMP-10 Conditioned Media

We used a retroviral gene delivery system to generate BMP-10-expressing cells. To generate the BMP-10 expression construct, the coding region of the mouse BMP-10 cDNA was subcloned into 5′ end of IRES-GFP cassette of a retroviral-based expression vector (MIEG3) (Williams et al., 2000). The viral packaging and the transduction of NIH3T3 cells were performed as previously described (Williams et al., 2000). Transduced cells were kept in DMEM contained with 10% FBS for 3 days before sorting for GFP positives using FACSVantage SE (Becton Dickinson). We used MIEG3 transduced/GFP positive cells as negative control. Northern blot analysis confirmed that BMP-10 transcript was only detected in MIEG3-BMP-10 transduced/GFP positive cells. To culture embryonic cardiomyocytes, BMP-10 conditioned media were collected from overnight cultures of BMP-10-expressing cells (BMP-10-NIH3T3) in DMEM containing 2% FBS. Control media were collected from overnight culture of control cells (MIEG3-NIH3T3) in DMEM containing 2% FBS. Embryonic cardiomyocytes were isolated from E13.5 and cultured in one-well Lab-Tek chamber slides for 48 hr. To assess the proliferative activity of cultured cells, cells were labeled with ^{3}H-thymidine (1 μCi/ml) for 2 hr before terminating the culture and fixed in methanol and processed for autoradiography and Periodic

Acid-Schiff (PAS) staining. The DNA labeling index of PAS-positive cells (cardiomyocytes) were recorded and compared between experimental and control groups.

Generation of ANF-BMP-10 Transgenic Mice

For details, see Supplemental Data online.

Acknowledgments

We wish to thank Cameron Christman from the San Diego Supercomputer Center for his help with the 3D reconstruction of the AVN. We thank Stephen McMullen from Cancer Center for his excellent assistance with microscopy, Sabina Kupershmidt and Dan Roden for mink-LacZ mice. Julie Anderson and Kim Weldy provided excellent maintenance of the mouse colony. Masa Hoshijima, Yibing Qyang, and Ju Chen provided help with the preparation and critical reading of this manuscript. This work was supported by funding from the NHLBI.

Received: February 20, 2003
Revised: February 3, 2004
Accepted: March 9, 2004
Published: April 29, 2004

References

Agard, D.A., Hiraoka, Y., Shaw, P., and Sedat, J.W. (1989). Fluorescence microscopy in three dimensions. Methods Cell Biol. *30*, 353–377.

Anderson, R.H., and Ho, S.Y. (2001). Anatomic criteria for identifying the components of the axis responsible for atrioventricular conduction. J. Cardiovasc. Electrophysiol. *12*, 1265–1268.

Anderson, R.H., Janse, M.J., van Capelle, F.J., Billette, J., Becker, A.E., and Durrer, D. (1974). A combined morphological and electrophysiological study of the atrioventricular node of the rabbit heart. Circ. Res. *35*, 909–922.

Azene, E.M., Xue, T., and Li, R.A. (2003). Molecular basis of the effect of potassium on heterologously expressed pacemaker (HCN) channels. J. Physiol. *547*, 349–356.

Benson, D.W., Silberbach, G.M., Kavanaugh-McHugh, A., Cottrill, C., Zhang, Y., Riggs, S., Smalls, O., Johnson, M.C., Watson, M.S., Seidman, J.G., et al. (1999). Mutations in the cardiac transcription factor NKX2.5 affect diverse cardiac developmental pathways. J. Clin. Invest. *104*, 1567–1573.

Biel, M., Schneider, A., and Wahl, C. (2002). Cardiac HCN channels: structure, function, and modulation. Trends Cardiovasc. Med. *12*, 206–212.

Bruneau, B.G. (2002). Transcriptional regulation of vertebrate cardiac morphogenesis. Circ. Res. *90*, 509–519.

Bruneau, B.G., Nemer, G., Schmitt, J.P., Charron, F., Robitaille, L., Caron, S., Conner, D.A., Gessler, M., Nemer, M., Seidman, C.E., and Seidman, J.G. (2001). A murine model of Holt-Oram syndrome defines roles of the T-box transcription factor Tbx5 in cardiogenesis and disease. Cell *106*, 709–721.

Chen, J., Kubalak, S.W., and Chien, K.R. (1998). Ventricular muscle-restricted targeting of the RXRalpha gene reveals a non-cell-autonomous requirement in cardiac chamber morphogenesis. Development *125*, 1943–1949.

Chen, F., Kook, H., Milewski, R., Gitler, A.D., Lu, M.M., Li, J., Nazarian, R., Schnepp, R., Jen, K., Biben, C., et al. (2002). Hop is an unusual homeobox gene that modulates cardiac development. Cell *110*, 713–723.

Chen, H., Shi, S., Lourdes, A., Li, W., Lu, J.T., Chen, Z., Yang, Z., Schneider, M.D., Chien, K.R., Conway, S.J., et al. (2004). BMP-10 is essential for maintaining cardiac growth during murine cardiogenesis. Development *131*, 2219–2231.

Crick, S.J., Anderson, R.H., Ho, S.Y., and Sheppard, M.N. (1999a). Localisation and quantitation of autonomic innervation in the porcine heart II: endocardium, myocardium and epicardium. J. Anat. *195*, 359–373.

Crick, S.J., Sheppard, M.N., Ho, S.Y., and Anderson, R.H. (1999b). Localisation and quantitation of autonomic innervation in the porcine heart I: conduction system. J. Anat. *195*, 341–357.

El-Badawi, A., and Schenk, E.A. (1967). Histochemical methods for separate, consecutive and simultaneous demonstration of acetylcholinesterase and norepinephrine in cryostat sections. J. Histochem. Cytochem. *15*, 580–588.

Elliott, D.A., Kirk, E.P., Yeoh, T., Chandar, S., McKenzie, F., Taylor, P., Grossfeld, P., Fatkin, D., Jones, O., Hayes, P., et al. (2003). Cardiac homeobox gene NKX2–5 mutations and congenital heart disease: associations with atrial septal defect and hypoplastic left heart syndrome. J. Am. Coll. Cardiol. *41*, 2072–2076.

Epstein, J.A. (2001). Developing models of DiGeorge syndrome. Trends Genet. *17*, S13–S17.

Franco, D., and Icardo, J.M. (2001). Molecular characterization of the ventricular conduction system in the developing mouse heart: topographical correlation in normal and congenitally malformed hearts. Cardiovasc. Res. *49*, 417–429.

Garg, V., Kathiriya, I.S., Barnes, R., Schluterman, M.K., King, I.N., Butler, C.A., Rothrock, C.R., Eapen, R.S., Hirayama-Yamada, K., Joo, K., et al. (2003). GATA4 mutations cause human congenital heart defects and reveal an interaction with TBX5. Nature *424*, 443–447.

Gassmann, M., Casagranda, F., Orioli, D., Simon, H., Lai, C., Klein, R., and Lemke, G. (1995). Aberrant neural and cardiac development in mice lacking the ErbB4 neuregulin receptor. Nature *378*, 390–394.

Goldmuntz, E., Geiger, E., and Benson, D.W. (2001). NKX2.5 mutations in patients with tetralogy of fallot. Circulation *104*, 2565–2568.

Gourdie, R.G., Severs, N.J., Green, C.R., Rothery, S., Germroth, P., and Thompson, R.P. (1993). The spatial distribution and relative abundance of gap-junctional connexin40 and connexin43 correlate to functional properties of components of the cardiac atrioventricular conduction system. J. Cell Sci. *105*, 985–991.

Gutierrez-Roelens, I., Sluysmans, T., Gewillig, M., Devriendt, K., and Vikkula, M. (2002). Progressive AV-block and anomalous venous return among cardiac anomalies associated with two novel missense mutations in the CSX/NKX2–5 gene. Hum. Mutat. *20*, 75–76.

Han, W., Bao, W., Wang, Z., and Nattel, S. (2002). Comparison of ion-channel subunit expression in canine cardiac Purkinje fibers and ventricular muscle. Circ. Res. *91*, 790–797.

Harvey, R.P., Lai, D., Elliott, D., Biben, C., Solloway, M., Prall, O., Stennard, F., Schindeler, A., Groves, N., Lavulo, L., et al. (2002). Homeodomain factor Nkx2–5 in heart development and disease. Cold Spring Harb. Symp. Quant. Biol. *67*, 107–114.

Hirota, H., Chen, J., Betz, U.A., Rajewsky, K., Gu, Y., Ross, J., Jr., Muller, W., and Chien, K.R. (1999). Loss of a gp130 cardiac muscle cell survival pathway is a critical event in the onset of heart failure during biomechanical stress. Cell *97*, 189–198.

Ho, S.Y., and Anderson, R.H. (2000). How constant anatomically is the tendon of Todaro as a marker for the triangle of Koch? J. Cardiovasc. Electrophysiol. *11*, 83–89.

Jenni, R., Oechslin, E., Schneider, J., Jost, C.A., and Kaufmann, P.A. (2001). Echocardiographic and pathoanatomical characteristics of isolated left ventricular non-compaction: a step towards classification as a distinct cardiomyopathy. Heart *86*, 666–671.

Kondo, R.P., Anderson, R.H., Kupershmidt, S., Roden, D.M., and Evans, S.M. (2003). Development of the cardiac conduction system as delineated by minK-lacZ. J. Cardiovasc. Electrophysiol. *14*, 383–391.

Kupershmidt, S., Yang, T., Anderson, M.E., Wessels, A., Niswender, K.D., Magnuson, M.A., and Roden, D.M. (1999). Replacement by homologous recombination of the minK gene with lacZ reveals restriction of minK expression to the mouse cardiac conduction system. Circ. Res. *84*, 146–152.

Lee, K.F., Simon, H., Chen, H., Bates, B., Hung, M.C., and Hauser, C. (1995). Requirement for neuregulin receptor erbB2 in neural and cardiac development. Nature *378*, 394–398.

Livak, K.J., and Schmittgen, T.D. (2001). Analysis of relative gene expression data using real-time quantitative PCR and the 2(-Delta Delta C(T)) method. Methods *25*, 402–408.

Lyons, I., Parsons, L.M., Hartley, L., Li, R., Andrews, J.E., Robb, L., and Harvey, R.P. (1995). Myogenic and morphogenetic defects in the heart tubes of murine embryos lacking the homeo box gene Nkx2–5. Genes Dev. *9*, 1654–1666.

Minamisawa, S., Wang, Y., Chen, J., Ishikawa, Y., Chien, K.R., and Matsuoka, R. (2003). Atrial chamber-specific expression of sarcolipin is regulated during development and hypertrophic remodeling. J. Biol. Chem. *278*, 9570–9575.

Nagy, A., Gocza, E., Diaz, E.M., Prideaux, V.R., Ivanyi, E., Markkula, M., and Rossant, J. (1990). Embryonic stem cells alone are able to support fetal development in the mouse. Development *110*, 815–821.

Neuhaus, H., Rosen, V., and Thies, R.S. (1999). Heart specific expression of mouse BMP-10 a novel member of the TGF-beta superfamily. Mech. Dev. *80*, 181–184.

Nguyen-Tran, V.T., Kubalak, S.W., Minamisawa, S., Fiset, C., Wollert, K.C., Brown, A.B., Ruiz-Lozano, P., Barrere-Lemaire, S., Kondo, R., Norman, L.W., et al. (2000). A novel genetic pathway for sudden cardiac death via defects in the transition between ventricular and conduction system cell lineages. Cell *102*, 671–682.

Pauli, R.M., Scheib-Wixted, S., Cripe, L., Izumo, S., and Sekhon, G.S. (1999). Ventricular noncompaction and distal chromosome 5q deletion. Am. J. Med. Genet. *85*, 419–423.

Rentschler, S., Zander, J., Meyers, K., France, D., Levine, R., Porter, G., Rivkees, S.A., Morley, G.E., and Fishman, G.I. (2002). Neuregulin-1 promotes formation of the murine cardiac conduction system. Proc. Natl. Acad. Sci. USA *99*, 10464–10469.

Ruiz-Lozano, P., and Chien, K.R. (2003). Cre-constructing the heart. Nat. Genet. *33*, 8–9.

Schott, J.J., Benson, D.W., Basson, C.T., Pease, W., Silberbach, G.M., Moak, J.P., Maron, B.J., Seidman, C.E., and Seidman, J.G. (1998). Congenital heart disease caused by mutations in the transcription factor NKX2–5. Science *281*, 108–111.

Sedmera, D., Reckova, M., DeAlmeida, A., Coppen, S.R., Kubalak, S.W., Gourdie, R.G., and Thompson, R.P. (2003). Spatiotemporal pattern of commitment to slowed proliferation in the embryonic mouse heart indicates progressive differentiation of the cardiac conduction system. Anat. Rec. *274A*, 773–777.

Shin, C.H., Liu, Z.P., Passier, R., Zhang, C.L., Wang, D.Z., Harris, T.M., Yamagishi, H., Richardson, J.A., Childs, G., and Olson, E.N. (2002). Modulation of cardiac growth and development by HOP, an unusual homeodomain protein. Cell *110*, 725–735.

St Amand, T.R., Zhang, Y., Semina, E.V., Zhao, X., Hu, Y., Nguyen, L., Murray, J.C., and Chen, Y. (2000). Antagonistic signals between BMP4 and FGF8 define the expression of Pitx1 and Pitx2 in mouse tooth-forming anlage. Dev. Biol. *217*, 323–332.

Tanaka, M., Chen, Z., Bartunkova, S., Yamasaki, N., and Izumo, S. (1999). The cardiac homeobox gene Csx/Nkx2.5 lies genetically upstream of multiple genes essential for heart development. Development *126*, 1269–1280.

Thomas, P.S., Kasahara, H., Edmonson, A.M., Izumo, S., Yacoub, M.H., Barton, P.J., and Gourdie, R.G. (2001). Elevated expression of Nkx-2.5 in developing myocardial conduction cells. Anat. Rec. *263*, 307–313.

Williams, D.A., Tao, W., Yang, F., Kim, C., Gu, Y., Mansfield, P., Levine, J.E., Petryniak, B., Derrow, C.W., Harris, C., et al. (2000). Dominant negative mutation of the hematopoietic-specific Rho GTPase, Rac2, is associated with a human phagocyte immunodeficiency. Blood *96*, 1646–1654.